Numerical Analysis of Protective Performance of Segmented Excavation Schemes for Metro Tunnels Considering Excavation-Induced Disturbance

Dingxiong Lin[1], Ruhui Lin[1], Shaowen Zhou[1], Hengyu Wang[2,3,4,*], Yongsheng Xiao[5], Jianjiang Bao[1] and Li Fei[1]

[1] Hongrun Construction Group Co., Ltd., Ningbo, 315100, China

[2] College of Civil and Architectural Engineering, NingboTech University, Ningbo, 315100, China

[3] College of Environmental Science and Engineering, Nankai University, Tianjin, 300110, China

[4] Institute of Wenzhou, Zhejiang University, Wenzhou, 325036, China

[5] Construction Branch, Ningbo Rail Transit Group Co., Ltd., Ningbo, 315100, China

INFORMATION

Keywords:
Artificially disturbed soil
disturbance zone
pit excavation
segmented excavation
metro tunnel

DOI: 10.23967/j.rimni.2025.10.66631

Revista Internacional de Métodos Numéricos para Cálculo y Diseño en Ingeniería

Numerical Analysis of Protective Performance of Segmented Excavation Schemes for Metro Tunnels Considering Excavation-Induced Disturbance

Dingxiong Lin[1], Ruhui Lin[1], Shaowen Zhou[1], Hengyu Wang[2,3,4,*], Yongsheng Xiao[5], Jianjiang Bao[1] and Li Fei[1]

[1]Hongrun Construction Group Co., Ltd., Ningbo, 315100, China

[2]College of Civil and Architectural Engineering, NingboTech University, Ningbo, 315100, China

[3]College of Environmental Science and Engineering, Nankai University, Tianjin, 300110, China

[4]Institute of Wenzhou, Zhejiang University, Wenzhou, 325036, China

[5]Construction Branch, Ningbo Rail Transit Group Co., Ltd., Ningbo, 315100, China

ABSTRACT

This paper presents an integrated laboratory and numerical study on the effects of excavation-induced soil disturbance on the displacement of underlying metro tunnels, as well as the protective performance of different segmented excavation methods. Artificial disturbed soils were prepared by mixing salt grains and different cement contents into remolded Ningbo silty clay. One-dimensional compression tests and triaxial shear tests were then conducted. These tests were used to investigate and compare the engineering properties of undisturbed and artificially disturbed soils. Subsequently, the Hardening Soil Model with Small Strain (HSS) parameters were obtained for soils under varying degrees of disturbance. Considering the deterioration of soil properties due to disturbance and based on the disturbance zoning determined from the unloading influence depth and field measurements, numerical simulations were performed using Plaxis 3D. These simulations analyzed tunnel displacements induced by large-area direct excavation and three segmented excavation schemes. The results indicate that excavation-induced disturbance can significantly increase tunnel vertical displacement. Compared to unmitigated direct excavation, segmented excavation methods (i.e., block jumping excavation, ends to center excavation, and sequential excavation) can reduce the average tunnel displacement by about 28%. Among the three schemes, block jumping excavation offers the best balance between deformation control and efficiency with the highest comprehensive benefit index (11.04%). Ends to center excavation provides optimal deformation control but exhibits relatively low efficiency. In contrast, although sequential excavation effectively reduces displacement, it leads to concentrated deformation and low construction efficiency, making it the least favorable option.

OPEN ACCESS

Received: 13/04/2025

Accepted: 30/07/2025

Published: 22/09/2025

DOI
10.23967/j.rimni.2025.10.66631

Keywords:
Artificially disturbed soil
disturbance zone
pit excavation
segmented excavation
metro tunnel

*Correspondence: Hengyu Wang (wanghy918@zju.edu.cn).

1 Introduction

The interaction between foundation pit excavation and tunnel construction is a research focus in geotechnical engineering. Tunneling activities causes ground movement from stress release, requiring assessment of its impact on nearby structures [1]. Likewise, pit excavation induces stress redistribution due to unloading, potentially leading to additional displacement of underlying tunnels [2,3]. With the rapid development of urban rail transit and underground space utilization in recent years, foundation pit excavation adjacent to existing metro tunnels has become increasingly common [4,5]. Currently, most metro tunnels are constructed using the shield method, and the tunnel structure is assembled using prefabricated segments through bolts, with several joints that exhibit weak integrity and low overall stiffness [6]. This makes metro tunnels particularly sensitive to deformation, and excessive deformation may lead to cracking or failure of tunnel lining segments [7]. Therefore, it is critical to adopt protective measures to limit tunnel displacement when conducting excavation projects adjacent to existing tunnels.

The segmented excavation method has been extensively applied in excavation projects throughout China. It has demonstrated strong effectiveness in controlling both foundation pit deformation and the associated deformation of adjacent metro tunnels [8–11]. The technical principle of segmented excavation involves dividing the original large foundation pit into construction areas for independent construction, considering the space–time effect of foundation pit excavation, and reducing the excavation-induced environmental deformation by reducing the excavation area, shortening the excavation exposure time, and setting up support in time [12] For tunnels affected by adjacent foundation pit excavation, dividing a large foundation pit into smaller sections can effectively reduce the impact on the tunnel. Currently, three commonly used segmented excavation methods are employed: (1) piano-playing-type interval excavation, also known as block jumping excavation [13]; (2) excavation from both ends toward the center, i.e., Ends to center excavation method [9,14,15]; and (3) sequential excavation from one end to the other [8]. However, current research has not yet conducted a comparative analysis of the characteristics of different segmented excavation methods and their protective effectiveness on metro tunnels.

Zhejiang Province is located in a developed coastal region characterized by soft marine soils. These coastal soft soils exhibit five prominent features, namely widespread sedimentation, high water content, high compressibility, low strength, and particularly strong structure. The structural integrity of such soils is especially pronounced; once disturbed, its structure is severely damaged and difficult to recover, significantly influencing the soil's mechanical properties. Numerous scholars have conducted research on construction-induced soil disturbances through laboratory experiments and field monitoring. Hardin and Drnevich [16] utilized resonant column tests and found that even slight disturbances could alter the initial modulus of soils significantly. Chung et al. [17] and Nagaraj et al. [18] conducted compression tests on soft clays and demonstrated that disturbance leads to a gradual degradation of the soil's structure, resulting in increased compressibility; once the soil structure is fully destroyed, its compression curve closely resembles that of remolded soil. Chen et al. [19] performed field tests and laboratory analyses on disturbed soils at the bottom of the Xianghu Station excavation pit collapse site in Hangzhou, and concluded that the soil strength at the pit bottom decreased by 40% to 80%. Additionally, Kimura and Saitoh [20] investigated the disturbance effects caused by vane insertion during vane shear tests on normally consolidated cohesive soils. They demonstrated that insertion-induced disturbance can lead to an underestimation of undrained shear strength by up to 20%–45%. The deterioration of soil engineering properties caused by excavation-induced disturbance also adversely affects the structural safety of underlying tunnels. Previous studies have indicated that inadequate understanding of the changes in soil properties induced

by construction disturbances is among the primary causes of engineering issues in foundation pits and tunnels [21].

Currently, existing studies primarily focus on the influence of construction-induced soil disturbance on either foundation pit engineering or tunnel engineering individually. However, research specifically addressing the effects of construction-induced soil disturbance from foundation pit excavation on adjacent tunnels is relatively limited. Dong [22] examined the disturbance effects induced during diaphragm wall construction on surrounding soil and adjacent structures. Lu et al. [23] performed finite element analyses to investigate the influence of soil disturbance on basal heave at the bottom of excavations. Zhu et al. [24] carried out three-dimensional finite element analyses to assess the disturbance effects of diaphragm wall installation on surrounding soils and adjacent buildings. Wei et al. [25] developed a mechanical model using Mindlin's solution to quantify additional stress on nearby tunnel shafts due to pit excavation unloading.

Regarding studies specifically focusing on the effects of foundation pit excavation-induced disturbance on existing tunnels, Hu et al. [26] defined the soil beneath the pit bottom as the disturbed zone and numerically analyzed the impacts of excavation construction on adjacent tunnels. Wang et al. [27], through numerical modeling, defined the entire excavation area as a disturbed zone and investigated the influences of foundation pit excavation on nearby tunnels. Based on these studies, it is clear that research concerning the impacts of deep foundation pit excavation considering construction-induced disturbance on adjacent underlying tunnels remains insufficient. Existing studies have not explored the influence of segmented excavation-induced disturbance on the effectiveness of protective measures for metro tunnels. Given that such excavation inevitably disturbs surrounding soil and influences tunnel performance, evaluating the protective effectiveness of segmented excavation methods under construction-induced disturbance is of significant practical value.

In our recent research, based on the unloading ratio and field disturbance tests conducted at the Gaotangqiao metro station excavation site in Ningbo, the pit bottom and retaining wall sides were classified as strong and weak disturbance zones, respectively. Based on a practical engineering project in Zhejiang province, the effects of excavation- and reinforcement-induced disturbances on the underlying tunnel were analyzed using Plaxis 3D, and the influence of soil reinforcement construction on the protective performance for metro tunnels was systematically evaluated [28]. Extending our previous research, this study analyzes the effects of soil property degradation caused by excavation-induced disturbance on the displacement of underlying metro tunnels under conditions of large-area direct excavation and three segmented excavation schemes using the finite element software Plaxis 3D. Additionally, the protective effects of these three segmented excavation methods on metro tunnels are compared and evaluated.

2 Engineering Background

2.1 Engineering Overview

As shown in Fig. 1 [28], the practical foundation pit project located in Zhejiang Province consists of two sections (north and south zones), interconnected by a basement structure. The excavation area of the foundation pit is approximately 34,000 m^2, and the perimeter of the pit is about 960 m. Except for approximately 40 m at the southernmost end, designed with a single-level basement, the remainder of the site adopts a two-level basement structure. The bottom elevation of the two-level basement floor slab is −11.1 m, while that of the single-level basement floor slab is −6.7 m. A dual-line metro shield tunnel passes underneath the foundation pit, embedded within silty clay. The tunnel has an outer diameter of 6.2 m and an inner diameter of 5.5 m. The lining structure comprises precast

concrete segments with concrete grade C50, and the tunnel is buried at a depth of approximately 22.7 m below ground surface. The primary support system consists of large-diameter bored cast-in-place piles (ϕ1000@1400) combined with two reinforced concrete braces. To enhance water and soil retention, triple-axis cement mixing piles are additionally installed outside the bored piles.

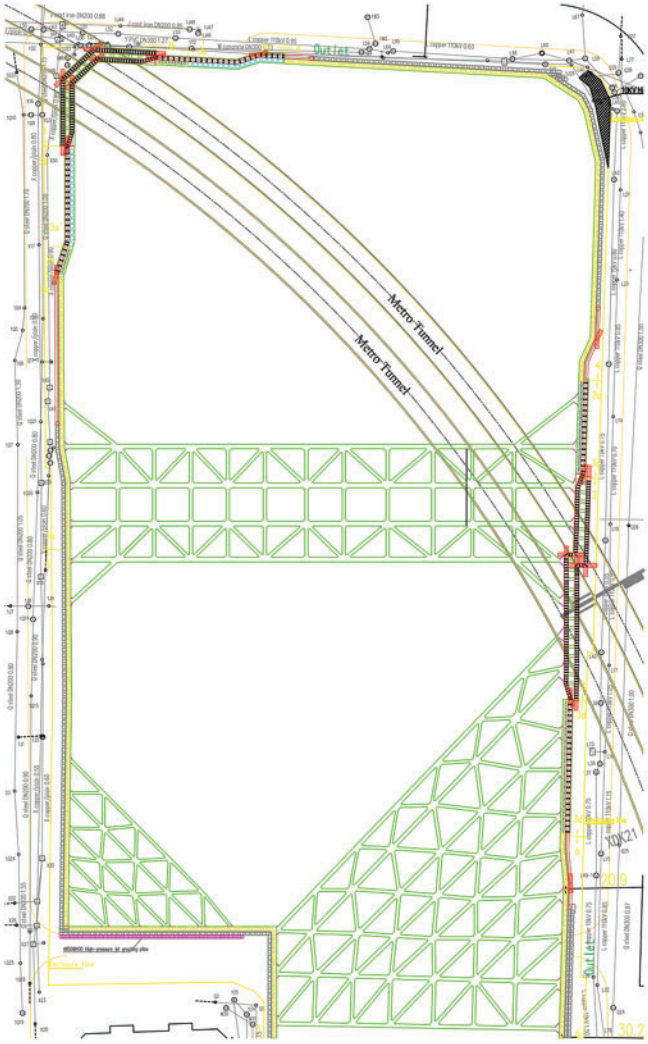

Figure 1: Plan view of the foundation pit and underlying dual-line tunnel (reproduced from Wang et al. [28], Scientific Reports, 2025, licensed under CC BY-NC-ND 4.0)

2.2 Segmented Excavation Methods

The minimum distance between the retaining piles of the excavation and the metro tunnel in this project is only 2 m, posing significant challenges for the construction of retaining structures and engineering piles. Previous studies have indicated that rationally designed excavation sequence and excavation size, by adequately considering spatial and temporal effects during excavation in soft soil, can effectively limit retaining wall deformation and ground surface settlement [12]. This approach ensures both the stability of the excavation and the safety of surrounding infrastructure and buildings during construction.

Proper selection of segmented excavation sequence can effectively control the basal rebound at the bottom of the excavation, thereby reducing its adverse influence on underlying tunnels. To investigate the effects of different segmented excavation sequences of soil layers on the metro tunnel structure, this study examines three excavation methods (i.e., block jumping excavation, ends to center excavation, and sequential excavation), following the principles of "segmentation, symmetry, and balance". As illustrated in Fig. 2, the excavation is first carried out uniformly to a depth of −4.9 m. Subsequently, the remaining soil above the tunnel is divided equally into 15 segments, each approximately 9.5 m wide. These 15 segments are then grouped from west to east into three excavation zones, labeled as Zones I, II, and III.

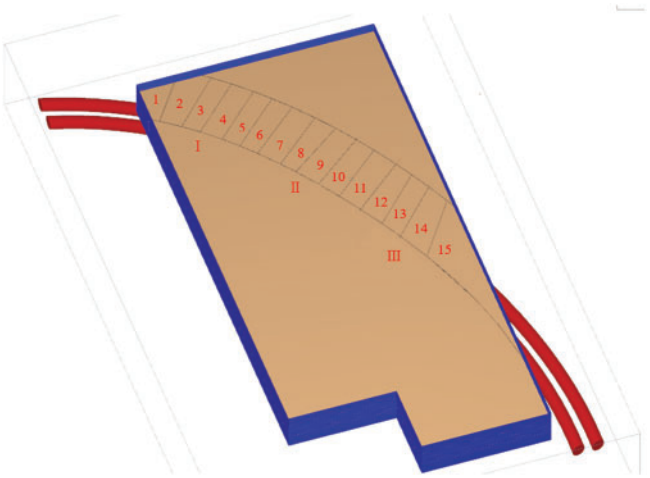

Figure 2: Schematic diagram of foundation pit excavation segmentation

2.2.1 Block Jumping Excavation

Fig. 3 illustrates the schematic of the block jumping excavation, in which excavation in the three designated zones begins simultaneously from the westernmost end. Using this excavation approach, the single-stage unloading volume is relatively large, and the excavation rate is faster. The soil mass above the tunnel is excavated in five stages, followed by the excavation of the remaining soil in the foundation pit in the sixth stage.

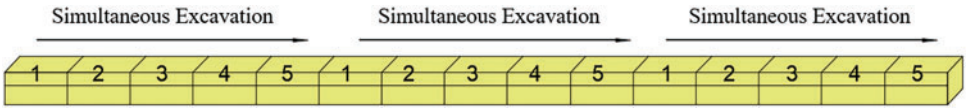

Figure 3: Schematic diagram of block jumping excavation

2.2.2 Ends to Center Excavation

Although the block jumping excavation allows for rapid construction, previous research has shown a clear positive correlation between soil unloading rate and tunnel uplift displacement. Due to the simultaneous excavation of large areas, significant unloading effects may occur. Therefore, an alternative excavation approach is proposed to reduce the single-stage excavation area and thus lower the unloading rate per excavation step. As depicted in Fig. 4, this method involves initially excavating

the soil at both ends above the tunnel, followed by excavation of the central region above the tunnel. The soil overlying the tunnel is removed in ten stages, with the remaining soil in the foundation pit excavated in the eleventh stage.

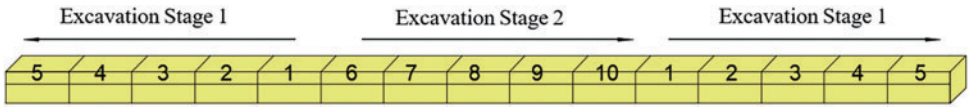

Figure 4: Schematic diagram of ends to center excavation

2.2.3 Sequential Excavation

In practical construction scenarios, simultaneous excavation on multiple working faces may be infeasible due to site conditions or limited construction personnel. Consequently, a sequential excavation method is adopted. As shown in Fig. 5, excavation proceeds sequentially from one end above the tunnel to the opposite end, with two segments excavated each time to maintain similar unloading rates per excavation. In this method, the soil above the tunnel is excavated in eight stages, followed by excavation of the remaining soil in the ninth stage. This sequential excavation method adheres primarily to the principle of segmentation and serves as a reference for comparison with the aforementioned excavation methods.

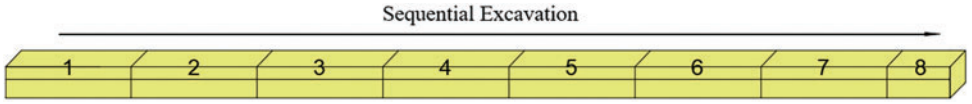

Figure 5: Schematic diagram of sequential excavation

Regardless of whether excavation is performed directly over a large area or conducted in segmented stages, soil disturbance inevitably occurs. Due to the high sensitivity of the soft soils surrounding the tunnel, such disturbance significantly reduces soil bearing capacity and induces continuous tunnel deformation. In this paper, analyses are conducted to investigate the effects of soil property degradation caused by excavation-induced disturbance on tunnel displacement, considering both large-area direct excavation and three segmented excavation schemes. Additionally, considering the construction-induced disturbance, the protective effects of these three segmented excavation methods on the metro tunnel are comparatively evaluated.

3 Disturbance Characterization and Laboratory Simulation

As shown in Fig. 6, to accurately simulate the impact of construction-induced disturbance on metro tunnels, a disturbance-based parameter transfer framework was developed. This framework systematically integrates field testing, laboratory simulation, and numerical modeling, ensuring a rational and data-supported transition from site conditions to model inputs.

The process begins with *in-situ* testing, including cone penetration tests (CPT), standard penetration tests (SPT), and shear wave velocity measurements, which are primarily used to evaluate the disturbance degree of soils behind the retaining structures. Meanwhile, the unloading influence depth is used to delineate the vertical extent of soil disturbance beneath the pit bottom. Based on both sources of information, the disturbance zones are classified into strong, weak, and non-disturbed regions. To represent these zones in the laboratory, artificially disturbed soils with controlled disturbance levels

are prepared by mixing remolded silty clay with varying cement contents and a fixed proportion of salt. The prepared specimens undergo one-dimensional compression tests and triaxial shear tests to determine key HSS (Hardening Soil Model with Small Strain) model parameters, such as the reference tangent modulus E_{oed}^{ref}, reference secant modulus E_{50}^{ref}, and the reference unloading-reloading modulus E_{ur}^{ref}. These parameters are then mapped to the corresponding disturbance zones and input into a numerical model (Plaxis 3D) in a spatially distributed manner. This enables the model to accurately capture the mechanical degradation of soils under excavation conditions. Ultimately, a numerical analysis is conducted to evaluate the impact of construction-induced disturbance on tunnel displacement under large-area direct excavation and three segmented excavation schemes, thereby enhancing the reliability of the simulation results and their applicability to practical engineering scenarios.

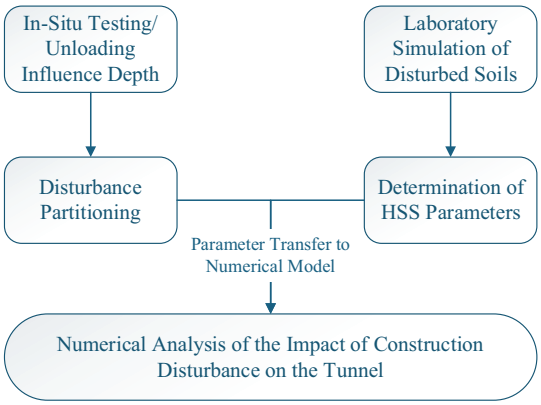

Figure 6: Disturbance-based parameter transfer framework

3.1 Construction Disturbance Partitioning

Foundation pit excavation causes soil disturbances both behind the retaining structures and beneath the pit bottom. In our research team's previous studies [28,29], based on the unloading influence depth and field measurements conducted at the Gaotangqiao metro excavation site in Ningbo, the disturbance zones induced by foundation pit excavation were delineated, as illustrated in Fig. 7 [28]. The soil disturbance is categorized into pit-bottom disturbance and disturbance behind the retaining structure: pit-bottom disturbance is divided into two zones, from the bottom of the pit to 1.25H excavation depth as a strong disturbance zone, and from 1.25H to 2.3H as a weak disturbance zone. Disturbance outside the retaining structure is divided into two zones, with the connection area between a depth of 1.4H beneath the ground surface and 1.0H outside the pit delineated as a strong disturbance zone, and the connection area between a depth of 2.0H beneath the ground surface and 2.0H outside the pit as a weak disturbance zone.

A comparison with field monitoring data showed that simulation results considering both strong and weak disturbance zones were more consistent with the measured values, confirming the rationality and accuracy of the zoning approach based on disturbance intensity [29].

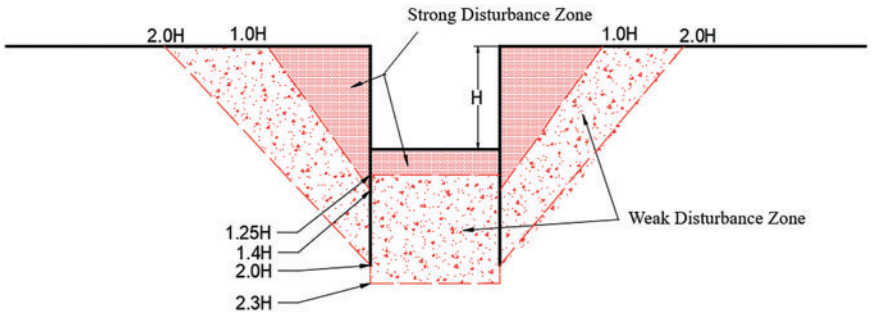

Figure 7: Diagram of disturbance zones (reproduced from Wang et al. [28], Scientific Reports, 2025, licensed under CC BY-NC-ND 4.0)

3.2 Laboratory Simulation of Soils with Varying Disturbance Degrees

The soil strata at the project site in Section 2.1 are representative of the typical soft soils prevalent in Zhejiang Province. Except for the mixed fill (Layer ①-0-1), plain fill (Layer ①-0-2), and clayey silt (Layer ②-1), the subsurface profile is predominantly composed of silty clay. To facilitate the analysis of construction-induced disturbances on tunnel displacement and the protective performance of segmented excavation measures, the subsequent investigation assumes a homogeneous silty clay layer encompassing the foundation pit enclosure and tunnel structure. The soil samples for laboratory testing were obtained from the ④-2 silty clay stratum at a depth of approximately 33 m, characterized by a dark gray color typical of deep soft soils in Zhejiang's coastal areas. The fundamental physical properties of the soil are summarized in Table 1.

Table 1: Basic physical properties indices of the ④-2 silty clay layer (reproduced from Wang et al. [28], Scientific Reports, 2025, licensed under CC BY-NC-ND 4.0)

Soil sample	Specific gravity	Moisture content/%	Bulk density (kN/m³)	Dry density (g/cm³)	Liquid limit/%	Plastic limit/%
Silty clay	2.73	39.9%	17.77	1.27	36	20

Due to the complexity of actual site conditions, it is challenging to obtain soil samples with identical disturbance levels. Carte and Liu [30] proposed that the difference between disturbed soil and undisturbed soil lies primarily in changes of soil structure. Wang et al. [27] validated the reliability and rationality of using artificial structured soils to simulate disturbed soils. The structural properties of soft soils arise primarily from interparticle bonding and fabric. The salt grains can act as temporary spacers, generating a macro-pore framework within the soil matrix during compaction. Upon saturation, the salt dissolves and is washed away, leaving behind a porous skeleton that mimics the macro-porosity typically found in naturally structured soft clays.

Referring to the research findings by Wang et al. [27], our recent research adopts the approach proposed by Nagaraj [31] to evaluate the disturbance degree of artificially disturbed soils with different cement contents based on their structural yield stresses obtained from one-dimensional compression tests, as summarized in Table 2 [28]. The cement content is defined as the ratio of the cement mass to the total mass of oven-dried natural soil and cement.

Table 2: Evaluation of disturbance degree of artificially disturbed soils (reproduced from Wang et al. [28], Scientific Reports, 2025, licensed under CC BY-NC-ND 4.0)

Sample	Structural yield stress/kPa	Disturbance degree
Natural Soil	132	0
2% Cement	127	4%
1.5% Cement	108	18%
1% Cement	80	40%
0.5% Cement	50	62%
Remolded soil	23	83%
Ideal remolded soil	0	100%

4 Numerical Analysis of the Impact of Construction Disturbance on the Tunnel

4.1 Parameter Settings

4.1.1 Soil Parameter Settings

In the study conducted by Lu et al. [23], field CPTU (Piezocone Penetration Tests) revealed that the degree of disturbance in the strongly disturbed areas was approximately 60%, while in the less disturbed areas, the disturbance level gradually decreased from 60% to 0% as the distance from the excavation site increased. Based on the disturbed soil obtained in Section 3.2, the disturbance level was set at 62% for the strongly disturbed areas and 40% for the less disturbed areas for the numerical analysis.

In this study, the soil behavior is represented using the Hardening Soil Model with Small Strain (HSS). The HSS model requires 11 standard Hardening Soil (HS) parameters and 2 additional small-strain parameters. As illustrated in Fig. 8, one-dimensional compression tests and triaxial shear tests were conducted to determine the HSS model parameters of soils with different disturbance degrees. The principal parameters of the HSS model have been established in our previous studies, as presented in Table 3 [28]. Notably, extensive research in Shanghai, China, has established a complete set of HSS model parameter selection methods for local soils, supported by experimental and monitoring data. Given the geographical proximity of Ningbo to Shanghai (approximately 150 km) and their similar geotechnical conditions within the Yangtze River Delta, this study adopts empirical formulas developed in Shanghai as a reference for determining G_0^{ref}. Previous studies indicate that for cohesive soils, G_0^{ref} typically ranges from 3.3 to 4.0 E_{ur}^{ref}, which has shown good agreement between measured and simulated results [32–35].

4.1.2 Pit and Tunnel Parameter Settings

The retaining piles, constructed with C30-grade concrete, are represented in the model using plate elements. The key parameters for the three-dimensional analysis of the retaining structure's plate elements are summarized in Table 4 [28].

The northern section of the project features two internal supports, each comprising 0.7 m × 0.9 m C30-grade reinforced concrete members. These supports are modeled using beam elements in the finite element analysis. The corresponding calculation parameters are presented in Table 5 [28].

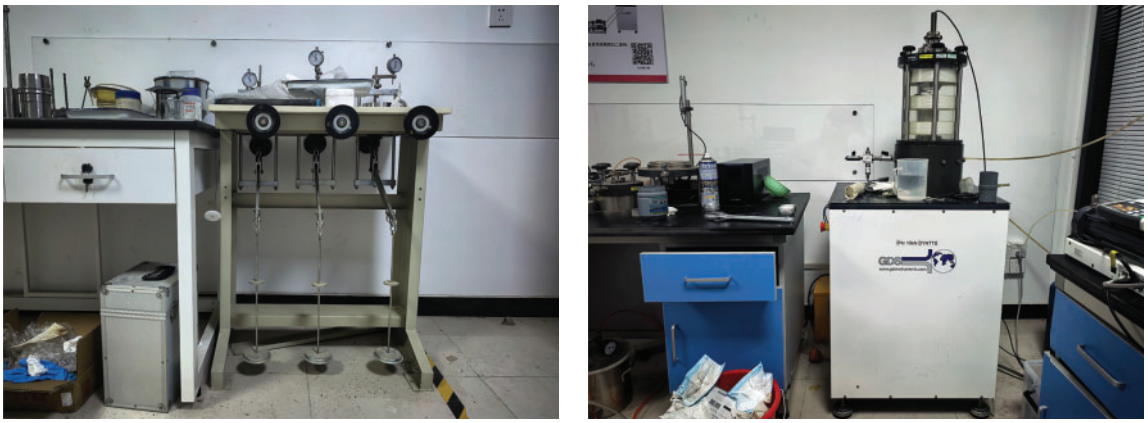

(**a**) (**b**)

Figure 8: Test equipment: (**a**) Triple-cell consolidation apparatus (Suzhou Top-Test Instrument Co., Ltd., Suzhou, China); (**b**) Triaxial apparatus (GDS Instruments, Global Digital Systems Ltd., Hampshire, UK)

Table 3: Main parameters of different disturbed soils (reproduced from Wang et al. [28], Scientific Reports, 2025, licensed under CC BY-NC-ND 4.0)

Disturbance	c'/kPa	φ'/°	E_{50}^{ref}/MPa	E_{ur}^{ref}/MPa	E_{oed}^{ref}/MPa	R_f	K_0	ν_{ur}	m	ψ/°	G_0^{ref}/MPa	$\gamma_{0.7}/10^{-4}$
62%	5.50	26	1.476	17.89	1.67	0.76	0.56	0.2	0.8	0	70.24	8.0
40%	6.88	24	1.546	22.40	1.95	0.81	0.59				78.40	7.7

Table 4: Equivalent parameters of retaining piles (reproduced from Wang et al. [28], Scientific Reports, 2025, licensed under CC BY-NC-ND 4.0)

Section size	Equivalent thickness d (m)	Elastic modulus E (kN/m^2)	Weight ω (kN/m^3)	Poisson's ratio ν
ϕ1000@1400	0.63	3×10^7	7	0.2

Table 5: Internal support parameters (reproduced from Wang et al. [28], Scientific Reports, 2025, licensed under CC BY-NC-ND 4.0)

Section size (mm)	Section area A (m^2)	Elastic modulus E (kN/m^2)	Compressive stiffness EA (kN)
700 × 900	0.63	3.0×10^7	1.89×10^7

The tunnel lining is made of C50-grade concrete with a unit weight of 15.5 kN/m^3. The tunnel lining parameters are detailed in Table 6 [28].

Table 6: Tunnel lining parameters (reproduced from Wang et al. [28], Scientific Reports, 2025, licensed under CC BY-NC-ND 4.0)

Section area A (m^2)	Equivalent thickness d (m)	Elastic modulus E_1 (kN/m^2)	Elastic modulus E_2 (kN/m^2)	Weight ω (kN/m^3)	Poisson's ratio ν
0.38	0.2611	5.8×10^6	2.59×10^7	15.5	0.2

4.2 Analysis Model

This paper primarily analyzes the impact of construction disturbances on underlying tunnels; therefore, only the northern excavation site is modeled. The numerical simulation model, based on an actual engineering project, is depicted in Fig. 9 [28]. The excavation area measures 238 m × 110 m, executed in four stages down to the pit bottom, with depths of 2.5, 4.9, 8.1, and 10.6 m, and supported at −1.9 and −4.9 m, respectively. The tunnel is a dual-track structure with a burial depth of −22.7 m.

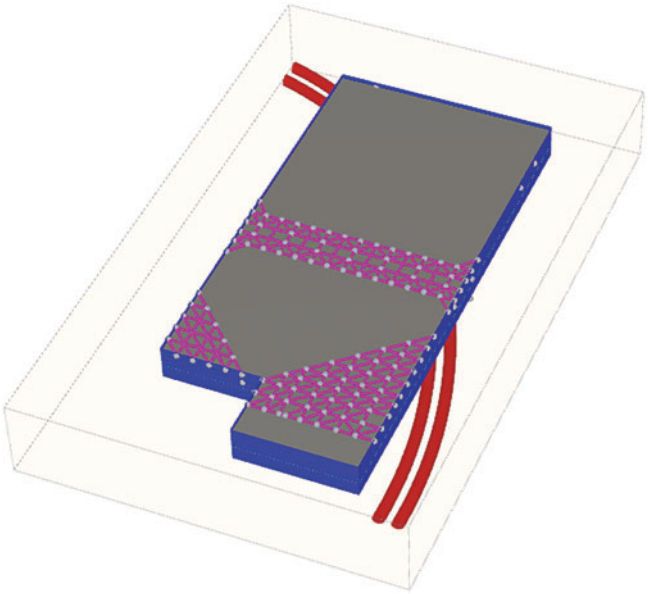

Figure 9: Model schematic (reproduced from Wang et al. [28], Scientific Reports, 2025, licensed under CC BY-NC-ND 4.0)

To analyze the effects of segmented excavation on the underlying tunnel, the soil directly above the tunnel is divided into zones, simulating a block and strip excavation method. As shown in Fig. 2, the excavation is first carried down to −4.9 m, after which the overlying soil of the tunnel is evenly divided into 15 segments, each approximately 9.5 m wide. These 15 segments are then divided from west to east into three excavation zones: I, II, and III. Excavation is carried out in two layers down to the bottom, with the first layer excavated down to an elevation of −8.1 m, and the second layer down to −10.6 m, followed by the excavation of other areas of the pit. After completing the segmented excavation to the bottom, the base slab is constructed promptly to control tunnel displacement.

In the numerical analysis, the effects of large-area direct excavation and three types of segmented excavation causing construction disturbances are considered. After each step of the segmented

excavation, the mechanical properties of the soil in the disturbed areas are degraded. According to the disturbance zoning in Section 3.1, the disturbed areas in the 3D model are set as shown in Fig. 10 [28].

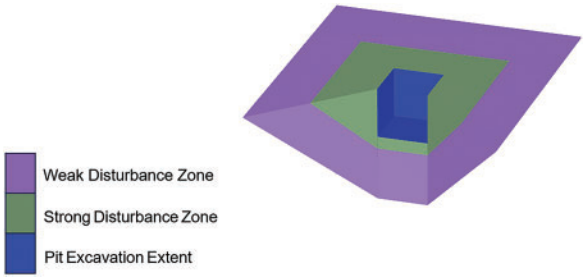

Figure 10: Schematic of the disturbance profile caused by pit excavation (reproduced from Wang et al. [28], Scientific Reports, 2025, licensed under CC BY-NC-ND 4.0)

The numerical analysis procedure adopted in this study consists of the following steps:

1. Initialization of the Geostress Field.
2. Resetting of Initial Displacements, Excavation of the Tunnel, and Activation of the Tunnel Lining.
3. Resetting of Initial Displacements and Activation of the Retaining Wall Plate Elements.
4. Excavation to a Depth of 2.5 m Below Ground Surface, Incorporating Soil Property Degradation within the Disturbance Zone and Installation of the First Support Level.
5. Continued Excavation to 4.9 m Depth, Incorporating Soil Property Degradation within the Disturbance Zone and Installation of the Second Support Level.
6. Further Excavation to 8.1 m, Incorporating Soil Property Degradation within the Disturbance Zone.
7. Final Excavation to the Pit Bottom at 10.6 m, Incorporating Soil Property Degradation within the Disturbance Zone.

4.3 Analysis Results

4.3.1 Impact of Large-Area Direct Excavation Disturbance on Tunnel Displacement

As shown in Fig. 11, our previous research demonstrated that when accounting for soil disturbance under large-area direct excavation, the maximum vertical displacement of the tunnel crown increases to 9.74 mm, compared to 8.23 mm without considering disturbance—an increase of 18.3%. In contrast, the horizontal displacement of the tunnel crown increases only slightly, from 3.92 to 4.08 mm, representing a 4.1% increase [28]. Excavation of the foundation pit above the tunnel leads to stress redistribution in the surrounding soil and generates additional upward stress at the pit bottom. The reduction in soil stiffness caused by construction-induced disturbance further amplifies the upward heave deformation at the pit bottom and the vertical deformation of the underlying existing subway tunnel. On one hand, the lateral confinement provided by the horizontal stress in the soil surrounding the tunnel reduces the influence of disturbance on horizontal displacement. On the other hand, the tunnel's horizontal extent lies primarily within a weakly disturbed zone, whereas the soil above the tunnel spans both weakly and strongly disturbed zones. Therefore, the impact of disturbance on vertical displacement is more significant than on horizontal displacement.

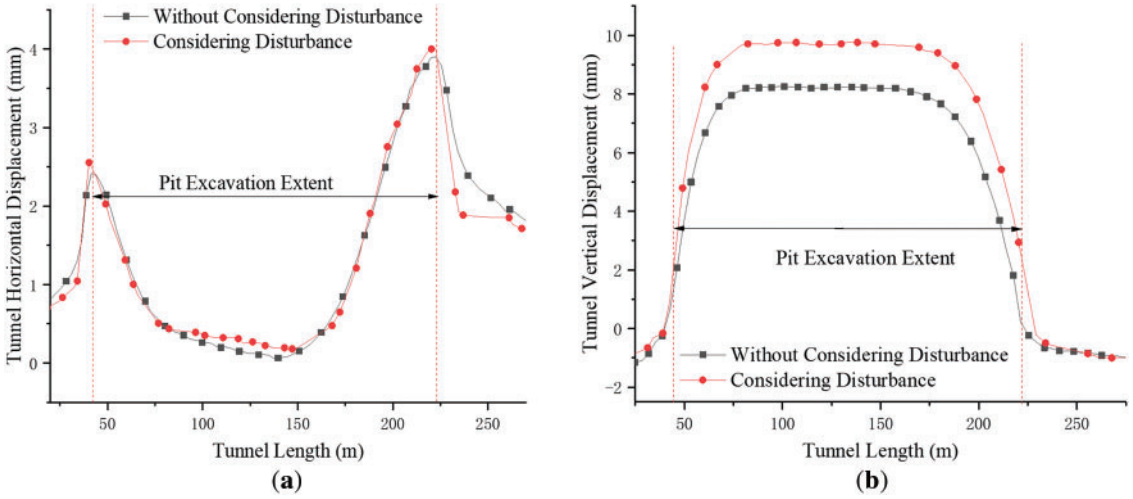

Figure 11: Tunnel displacement considering large-area direct excavation disturbance: (**a**) Tunnel horizontal displacement; (**b**) Tunnel vertical displacement (reproduced from Wang et al. [28], Scientific Reports, 2025, licensed under CC BY-NC-ND 4.0)

These results indicate that construction-induced disturbance has a more pronounced effect on vertical displacement than on horizontal displacement. Moreover, the displacement patterns of the two parallel tunnels are similar due to their close proximity [28]. Therefore, the subsequent analyses in this study focus primarily on the vertical displacement of the left-line tunnel, with the results obtained under disturbed conditions used for further analysis in the following sections. The term "unmitigated excavation" in the following text refers to large-area direct excavation.

4.3.2 Impact of Segmented Excavation Disturbance on Tunnel Displacement

Fig. 12 shows the vertical displacement curve of the tunnel during block jumping excavation. Before Step 5, the displacement curve of the tunnel is wavy, with displacement progressively increasing as the excavation progresses. Before the extensive unloading in Step 6, the maximum vertical displacement of the tunnel is 6.49 mm, which increases to 6.99 mm after the extensive unloading in Step 6. Compared to unmitigated excavation, the maximum vertical displacement of the tunnel is reduced by 28.2%.

In the block jumping excavation scheme, the three excavation zones begin simultaneously from the westernmost section. Due to the constraint imposed by the retaining structure, tunnel displacement increases slowly after the excavation of the first zone. In contrast, more rapid tunnel displacement growth is observed following the excavation of the second and third zones, resulting in two initial tunnel displacement peaks. As excavation progresses eastward, these peaks shift accordingly, and the overall tunnel deformation exhibits a wavy pattern. The soil retained around the tunnel provides a counterpressure, which mitigates abrupt changes in displacement. As a result, the deformation is more evenly distributed along the tunnel alignment, reducing localized stress concentrations and helping to minimize the risks of segment cracking, joint leakage, and overall structural degradation.

Fig. 13 shows the vertical displacement curve of the tunnel under ends to center excavation. The displacement curve is M-shaped; after the excavation of the end sections is completed, the maximum vertical displacement is about 6.20 mm. After the excavation reaches Step 10, the vertical displacement

of the tunnel reaches its maximum value before extensive unloading, at 6.62 mm. After extensive unloading in Step 11, the maximum vertical displacement of the tunnel is 7.13 mm, which is 26.8% lower compared to unmitigated excavation.

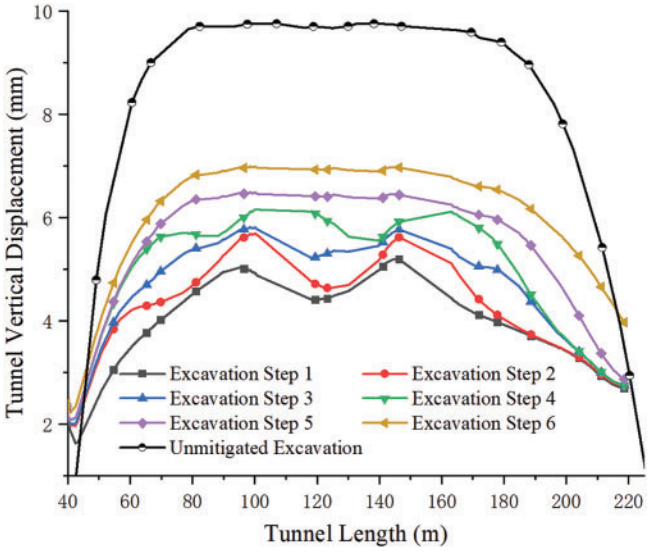

Figure 12: Impact of block jumping excavation on tunnel displacement considering soil disturbance

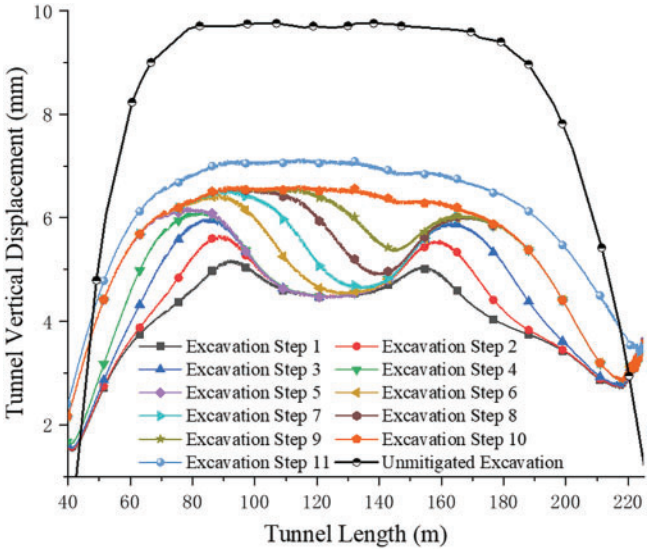

Figure 13: Impact of ends to center excavation on tunnel displacement considering soil disturbance

In the ends to center excavation scheme, the soil above both ends of the tunnel is excavated first, releasing the overburden stress and causing two initial peaks in vertical displacement near the tunnel ends. Meanwhile, the unexcavated soil at the center provides counterpressure, which effectively restrains displacement in the middle section of the tunnel. As a result, the tunnel initially exhibits an M-shaped deformation pattern, with the central section showing almost no change in displacement prior to the sixth excavation step. Once excavation of the central zone begins, the counterpressure

diminishes, and the vertical displacement at the tunnel crown starts to increase progressively. During this process, the location of the maximum displacement gradually shifts inward along the direction of excavation. Compared to block jumping excavation, this method leads to a slower and more controlled progression of tunnel deformation, which is beneficial for reducing the risk of sudden structural response and improving excavation safety.

Fig. 14 presents the vertical displacement curve of the tunnel under the sequential excavation scheme. The tunnel displacement increases rapidly, and by Step 5—prior to large-scale unloading—the vertical displacement of the tunnel reaches its maximum value of 6.5 mm, exhibiting a concentrated deformation distribution. After extensive unloading in Step 9, the maximum vertical displacement of the tunnel is 7 mm, which is 28.1% lower compared to unmitigated excavation.

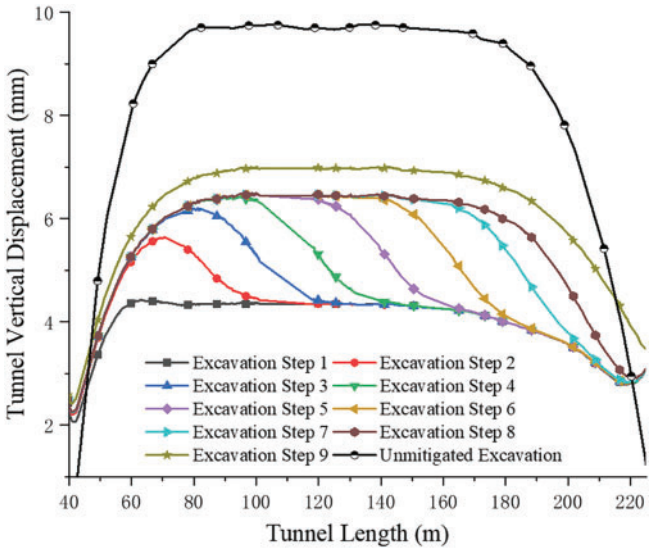

Figure 14: Impact of sequential excavation on tunnel displacement considering soil disturbance

In the sequential excavation scheme, tunnel displacement increases progressively and synchronously with the advancement of excavation. As the excavation moves forward, the location of maximum tunnel displacement also shifts in the same direction. This pattern results from the continuous release of stress in a single direction, which causes overlapping stress and displacement fields within the surrounding soil. The cumulative unloading effect leads to concentrated deformation, particularly in the rear portion of the excavation zone [36]. Such concentrated unloading is less favorable for deformation control and may increase the risk of structural issues such as segment cracking, leakage, and uneven settlement in the tunnel structure.

Fig. 15 shows the changes in tunnel displacement with each excavation step under different segmented excavation methods. In the final step, due to extensive unloading in the pit, the displacement of the tunnel increases significantly in all excavation methods. Since the amount of unloading is the same, the maximum displacement of the tunnel is approximately the same for all three methods, around 7 mm, which is about a 28% reduction compared to unmitigated excavation of 9.74 mm. Sequential excavation quickly reaches a displacement of about 6.5 mm due to the overlapping stresses caused by the excavation. The ends to center excavation and block jumping excavation have slower displacement growth due to the counterpressure of the soil layers, with ends to center excavation experiencing the

slowest displacement increase due to the smallest single unloading rate, but requiring more steps and more time for excavation.

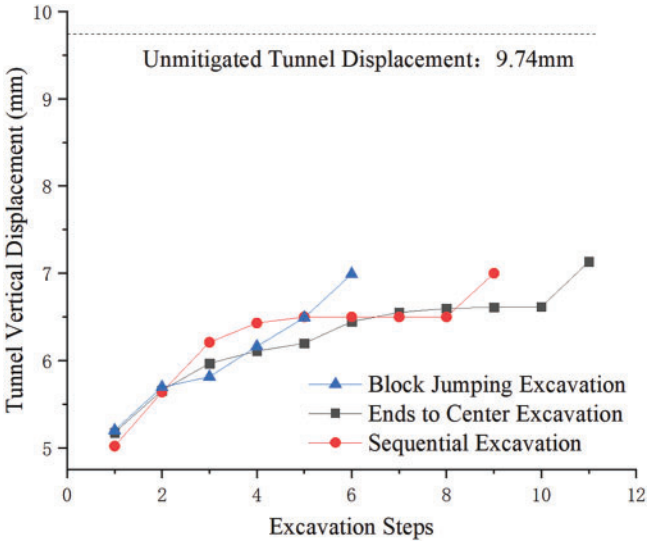

Figure 15: Tunnel displacement with each excavation step under different segmented excavation

The key indicators of the three segmented excavation methods are summarized in Table 7. The increases in construction duration and cost are calculated based on the assumption of renting 10 excavators for the project, with the cost increase considering only the additional machine rental expenses. To balance the differences in tunnel displacement, construction duration, and cost among the three excavation methods and to better guide practical engineering applications, a comprehensive benefit index is introduced to quantitatively evaluate the key indicators of each method.

$$I = \alpha\left(1 - \frac{D}{D_0}\right) + \beta\left(1 - \frac{T}{T_0}\right) + \gamma\left(1 - \frac{C}{C_0}\right) \tag{1}$$

where: D/D_0 = actual tunnel displacement/tunnel displacement without mitigation measures; T/T_0 = actual construction duration/baseline duration; C/C_0 = actual cost/baseline cost; The parameters α, β and γ represent the weighting coefficients for tunnel displacement, construction duration, and cost, respectively.

These coefficients (α, β and γ) represent the relative importance of tunnel displacement, construction duration, and cost, respectively. Importantly, they are adjustable and project-specific, depending on the engineering priorities of a particular project. In extreme cases, for instance, in high-priority metro projects where displacement control is paramount, it might even be reasonable to assign $\alpha = 1$ and $\beta = \gamma = 0$, prioritizing safety over time and cost.

Taking this project as an example, let $\alpha = 0.7$, $\beta = 0.2$, and $\gamma = 0.1$. The comprehensive benefit index of large-area direct excavation is taken as 0 for reference. Among the three segmented excavation methods, the comprehensive benefit indices of block jumping excavation, ends to center excavation, and sequential excavation are 11.04%, 0.86%, and −7.63%, respectively.

Table 7: Quantitative comparison of segmented excavation methods

Evaluation index	Block jumping excavation	Ends to center excavation	Sequential excavation
Maximum displacement reduction rate	28.2%	26.8%	28.1%
Displacement distribution	Suboptimal (wave-shaped)	Optimal (M-shaped)	Worst (concentrated)
Number of excavation steps	5 steps	10 steps	15 steps
Equipment utilization	High (3 working faces)	Medium (2 working faces)	Low (1 working face)
Construction duration increase (%)	+40%	+86%	+133%
Cost increase (%)	+7%	+7%	+7%
Comprehensive benefit index	11.04%	0.86%	−7.63%

The choice of excavation method should consider both deformation control and construction efficiency. Block jumping excavation is the most favorable option, offering the highest comprehensive benefit (+11.04%) due to its optimal displacement control effect (28.2% reduction), wave-like and evenly distributed deformation pattern, and efficient five-step construction process. However, this method involves a 40% increase in construction time and a 7% rise in equipment cost. Ends to center excavation method achieves a 26.8% reduction in displacement and produces an optimal M-shaped displacement distribution with slower growth of tunnel deformation. However, the 10-step construction process leads to an 86% increase in construction duration, resulting in a comprehensive benefit index of only 0.86%. Although sequential excavation achieves a maximum displacement reduction of 28.1%, the concentrated deformation distribution, 15-step construction process, and a 133% increase in construction time lead to a negative benefit index of −7.63%. Therefore, block jumping excavation is recommended as the primary option to ensure safety. The end to center method is suitable when displacement control is prioritized and extended construction timelines are acceptable, while the sequential method should be selected with caution. Similar research findings have also shown that ends to center excavation has a better effect on controlling pipeline settlement than sequential excavation [37].

5 Research Limitations

While this study provides meaningful insights into the effects of excavation-induced disturbance and the protective performance of segmented excavation schemes in silty clay strata, several limitations should be acknowledged.

First, the artificial disturbance simulation method adopted in laboratory testing—through controlled addition of cement and salt to remolded soil—may not fully replicate the complex mechanical and structural changes induced by actual construction activities. Moreover, the numerical model considers only the degradation of soil parameters due to disturbance and does not account for dynamic effects such as vibrations from excavation machinery and the lagging installation of support structures,

which may further influence soil behavior and tunnel responses during excavation. Although the methodology allows for quantifiable control of disturbance degree, the differences between laboratory-simulated and field-induced disturbance require further validation through *in-situ* comparisons.

Second, the current study focuses solely on silty clay deposits. The applicability of the proposed disturbance zoning method and HSS model parameters to other geotechnical formations—such as silt, silty soils, or stratified layers with varying stiffness—has not yet been verified. In particular, the interaction between multiple soil strata, which could affect the development and propagation of disturbance zones, was not considered and should be addressed in future research.

Third, the sensitivity of the disturbance effect to tunnel burial depth was not investigated. Tunnel depth may significantly influence the unloading path, disturbance propagation, and resulting deformations. Further parametric studies are needed to explore the role of burial depth in disturbance evolution and tunnel-soil interaction.

Lastly, while the disturbance zoning was informed by *in-situ* testing data and validated using field monitoring at the Gaotangqiao station, additional case studies and long-term field observations are necessary to generalize the findings and enhance the practical applicability of the proposed framework.

6 Conclusion

This paper, based on an actual project in Zhejiang Province and using Plaxis 3D, studied the effects of excavation-induced soil disturbance on the displacement of underlying metro tunnels, as well as the protective performance of different segmented excavation methods. The main conclusions are as follows:

(1) Segmented excavation methods significantly reduce tunnel displacement and improve deformation characteristics. Compared to unmitigated excavation, the maximum vertical displacement of the tunnel is reduced by an average of 27.7% in the three segmented excavation methods (i.e., block jumping excavation, ends to center excavation, and sequential excavation), with the final displacement controlled at about 7 mm.

(2) Block jumping and ends to center excavation schemes offer better deformation control than sequential excavation. The ends to center excavation, due to the counterpressure from the retained central soil, has the slowest displacement growth and an M-shaped distribution; block jumping excavation ensures more uniform displacement development through retained soil counterpressure; whereas sequential excavation, due to concentrated stress, has the fastest displacement increase, reaching 6.5 mm by Step 5, offering the weakest protection for the tunnel.

(3) In engineering practice, the selection of the most appropriate segmented excavation method should consider tunnel deformation control requirements, project schedule constraints, equipment availability, and overall cost. A quantitative comparison of three segmented excavation methods reveals that block jumping excavation delivers the best overall performance, achieving a significant displacement reduction (28.2%) and the highest comprehensive benefit index (11.04%). The ends to center method provides a balanced approach to deformation control but results in a considerable extension of the schedule. Although sequential excavation reduces displacement effectively, it causes concentrated deformation and suffers from low construction efficiency, making it the least favorable option.

(4) This study is based on numerical simulations and disturbance degree evaluation in silty clay strata; however, its applicability to other common geological conditions such as silt,

silty soils, and multilayered formations remains unverified. Although disturbance zones were classified into strong, weak, and non-disturbed areas based on *in-situ* testing data from similar local projects, further investigation is needed to accurately define the extent and intensity of excavation-induced disturbance under varied geological and construction conditions. In particular, the influence of different excavation techniques on disturbance zones requires in-depth analysis. Moreover, the impact of tunnel burial depth on the development and distribution of disturbance zones has not been fully explored and warrants further study. Future work should include field validation of the artificial disturbance simulation to improve the reliability and practical applicability of the proposed methods.

Acknowledgement: Not applicable.

Funding Statement: This research was funded by Zhejiang Provincial Natural Science Foundation of China (Grant No. LHZ23E080002), and Zhejiang Province Construction Research Project (Grant No. 2023K225).

Author Contributions: The authors confirm contribution to the paper as follows: Conceptualization, Dingxiong Lin and Ruhui Lin; methodology, Hengyu Wang; software, Hengyu Wang; validation, Shaowen Zhou; formal analysis, Hengyu Wang; investigation, Hengyu Wang and Yongsheng Xiao; writing—original draft preparation, Hengyu Wang; writing—review and editing, Jianjiang Bao and Li Fei; visualization, Hengyu Wang; supervision, Ruhui Lin; project administration, Dingxiong Lin; funding acquisition, Hengyu Wang and Dingxiong Lin. All authors reviewed the results and approved the final version of the manuscript.

Availability of Data and Materials: The authors confirm that the data supporting the findings of this study are available within the article.

Ethics Approval: Not applicable.

Conflicts of Interest: The authors declare no conflicts of interest to report regarding the present study.

References

1. Soomro MA, Dai ML, Cui ZD, Mangi N, Mangnejo DA, Zhao CY. Impact of twin stacked tunnels on laterally loaded pile groups: an emphasis on settlement and load transfer mechanisms using centrifuge and numerical modelling. Structures. 2024;70:107746. doi:10.1016/j.istruc.2024.107746.
2. Liu B, Wu WW, Lu HP, Chen S, Zhang DW. Effect and control of foundation pit excavation on existing tunnels: a state-of-the-art review. Tunn Undergr Space Technol. 2024;147:105704. doi:10.1016/j.tust.2024.105704.
3. Soomro MA, Mangnejo DA, Saand A, Mangi N, Auchar Zardari M. Influence of stress relief due to deep excavation on a brick masonry wall: 3D numerical predictions. Eur J Environ Civ Eng. 2022;26(15):7621–44. doi:10.1080/19648189.2021.2004450.
4. Meng FY, Chen RP, Xu Y, Wu K, Wu HN, Liu Y. Contributions to responses of existing tunnel subjected to nearby excavation: a review. Tunn Undergr Space Technol. 2022;119:104195. doi:10.1016/j.tust.2021.104195.
5. Vinoth M, Aswathy MS. Behaviour of existing tunnel due to adjacent deep excavation—a review. Int J Geotech Eng. 2022;16(9):1132–51. doi:10.1080/19386362.2021.1952800.

6. Shi CH, Cao CY, Lei MF, Peng LM, Ai HJ. Effects of lateral unloading on the mechanical and deformation performance of shield tunnel segment joints. Tunn Undergr Space Technol. 2016;51:175–88. doi:10.1016/j.tust.2015.10.033.
7. Zhou FC, Zhou P, Li JF, Lin JY, Ge TC, Deng SM, et al. Deformation characteristics and failure evolution process of the existing metro station under unilateral deep excavation. Eng Fail Anal. 2022;131:105870. doi:10.1016/j.engfailanal.2021.105870.
8. Chiu HW, Hsu CF, Tsai FH, Chen SL. Influence of different construction methods on lateral displacement of diaphragm walls in large-scale unsupported deep excavation. Buildings. 2023;14(1):23. doi:10.3390/buildings14010023.
9. Fan S, Song Z, Xu T, Wang K, Zhang Y. Tunnel deformation and stress response under the bilateral foundation pit construction: a case study. Arch Civ Mech Eng. 2021;21:1–19.
10. Li MG, Zhang ZJ, Chen JJ, Wang JH, Xu AJ. Zoned and staged construction of an underground complex in Shanghai soft clay. Tunn Undergr Space Technol. 2017;67:187–200. doi:10.1016/j.tust.2017.04.016.
11. Tan Y, Wei B, Zhou X, Diao Y. Lessons learned from construction of Shanghai metro stations: importance of quick excavation, prompt propping, timely casting, and segmented construction. J Perform Constr Facil. 2015;29(4):04014096. doi:10.1061/(asce)cf.1943-5509.0000599.
12. Liu JH, Liu GB, Fan YQ. The theory and its practice by using the rule of time-space effect in soft soil excavation. Undergr Eng Tunn. 1999;(3):7–12+47. (In Chinese).
13. Li MG, Chen JJ, Wang JH, Zhu YF. Comparative study of construction methods for deep excavations above shield tunnels. Tunn Undergr Space Technol. 2018;71:329–39. doi:10.1016/j.tust.2017.09.014.
14. Tanoli AY, Yan B, Xiong YL, Ye GL, Khalid U, Xu ZH. Numerical analysis on zone-divided deep excavation in soft clays using a new small strain elasto-plastic constitutive model. Undergr Space. 2022;7(1):19–36. doi:10.1016/j.undsp.2021.04.004.
15. Xiao X, Chen JJ, Li MG, Wang JH. Field monitoring of an existing cut-and-cover tunnel between two large-scale deep excavations. J Aerosp Eng. 2018;31(6):04018082. doi:10.1061/(asce)as.1943-5525.0000851.
16. Hardin BO, Drnevich VP. Shear modulus and damping in soils: measurement and parameter effects. J Soil Mech Found Div. 1972;98(6):603–24. doi:10.1061/jsfeaq.0001756.
17. Chung SG, Kwag JM, Giao PH, Baek SH, Prasad KN. A study of soil disturbance of Pusan clays with reference to drilling, sampling and extruding. Geotechnique. 2004;54(1):61–5. doi:10.1680/geot.2004.54.1.61.
18. Nagaraj TS, Murthy BS, Vatsala A, Joshi RC. Analysis of compressibility of sensitive soils. J Geotech Eng. 1990;116(1):105–18. doi:10.1061/(asce)0733-9410(1990)116:1(105).
19. Chen YM, Hu Q, Chen RP. Soil disturbance by the collapse of retaining wall for a pit excavation and the induced additional settlement: a case study of Hangzhou Metro Xianghu Station. China Civ Eng J. 2014;47(7):110–7. (In Chinese).
20. Kimura T, Saitoh K. Effect of disturbance due to insertion on vane shear strength of normally consolidated cohesive soils. Soils Found. 1983;23(2):113–24. doi:10.3208/sandf1972.23.2_113.
21. Zhu JF. Study on properties of soil considering disturbance [dissertation]. Hangzhou, China: Zhejiang University; 2011.
22. Dong Y. Finite element investigation of ground response during diaphragm wall panel installation. Can Geotech J. 2023;60(12):1792–811. doi:10.1139/cgj-2022-0649.
23. Lu TS, Liu SY, Cai GJ, Wu K, Xia WJ. Study on the disturbance and recompression settlement of soft soil induced by foundation excavation. Rock Soil Mech. 2021;42(2):565–573+580. (In Chinese).
24. Zhu N, Zhou Y, Liu W, Shi PX, Wu B. Study of silty soil behavior disturbed for installation of diaphragm wall in Suzhou. Rock Soil Mech. 2018;39(S1):529–36. (In Chinese).
25. Wei X, Ma J, Wang X, Yan Z, Yan J, Wei G. Evaluation of the additional stress on adjacent tunnel shafts induced by foundation pit excavation. Adv Civ Eng. 2024;2024(1):6890483. doi:10.1155/2024/6890483.

26. Hu Q, Xu SF, Chen RP, Long R. Influence of soil disturbance on metro tunnel in soft clay due to excavation of deep foundation pit. Chin J Geotech Eng. 2013;35(S2):537–41. (In Chinese).
27. Wang C, Ling DS, Wang HY. Influence of soft clay structure on pit excavation and adjacent tunnels. J Zhejiang Univ Eng Sci. 2020;54(2):264–74. (In Chinese).
28. Wang HM, Lin MS, Li JB, Wang HY, Fu XF, Zhong CH. Effects of construction disturbances on tunnel displacement and the protective role of soil reinforcement in metro tunnels. Sci Rep. 2025;15(1):19780. doi:10.1038/s41598-025-04692-z.
29. Bai SY, Wang WJ, Xie XY, Zhu DL. Experimental study on HS-small model parameters of soil considering disturbance and its application in foundation pit engineering. Rock Soil Mech. 2023;44(1):206–16. (In Chinese).
30. Carter JP, Liu MD. Virgin compression of structured soils. Géotechnique. 1999;49(1):43–57. doi:10.1680/geot.1999.49.1.43.
31. Nagaraj TS. Analysis and assessment of sampling disturbance of soft sensitive clays. Géotechnique. 2003;53(7):679–83. doi:10.1680/geot.2003.53.7.679.
32. Wang WD, Li Q, Xu ZH, Zong LD, Li YL. Investigation and application of small-strain model parameters for soft clay deposits. Chin J Undergr Space Eng. 2023;19(3):844–55. (In Chinese).
33. Gu XQ, Wu RT, Liang FY, Gao GY. On HSS model parameters for Shanghai soils with engineering verification. Rock Soil Mech. 2021;42(3):833–45. (In Chinese).
34. Ministry of Housing and Urban-Rural Development of Shanghai City. Technical Code for Excavation Engineering. DG/TJ 508-61-2018. Shanghai, China: Tongji University Press; 2018.
35. Wang WD, Wang HR, Xu ZH. Study of parameters of HS-Small model used in numerical analysis of excavations in Shanghai area. Rock Soil Mech. 2013;34(6):1766–74. (In Chinese).
36. Ding Z, Zhang X, Jin JK, Zhong WL. Measurement analysis on whole excavation of foundation pit and deformation of adjacent metro tunnel. Rock Soil Mech. 2019;40(S1):415–23. (In Chinese).
37. Song ZP, Wu YC, Zhang YW, Wang KS, Tian JL, Tian XW. Deformation response of a pipeline to nearby deep foundation pit excavation: numerical simulations and field tests. Appl Sci. 2023;13(11):6597. doi:10.3390/app13116597.